X-ray reflectivity and diffuse-scattering study of $CoSi_2$ layers in Si produced by ion-beam synthesis

D. Bahr and W. Press
Universität Kiel, Institut für Experimentalphysik, Olshausenstrasse 40, D-2300 Kiel 1, Federal Republic of Germany

R. Jebasinski and S. Mantl
Forschungszentrum Jülich GmbH, Postfach 1913, D-5170 Jülich, Federal Republic of Germany
(Received 20 July 1992)

Buried single crystalline layers of $CoSi_2$ in Si with (001) and (111) surfaces were produced by ion-beam synthesis. Depending on the annealing procedure, surface orientation, and ion dose, different results in interface quality are achieved. X-ray experiments under grazing incidence conditions (specular and diffuse scattering) are used for the investigation of their properties. We present a quantitative evaluation of the diffuse scattering underneath the specular reflectivity for multilayer systems with strongly varying electron densities.

I. INTRODUCTION

For device fabrication in microelectronics increasing demands exist for the production of thin films with high quality. Especially low electric resistance, high-temperature stability, and the possibility of generating 100-nm-thick structures with sharp interfaces over long lateral ranges in the technically relevant (100) surface become important. Within this scope the metallic $CoSi_2$ is an interesting material. Its specific electric resistance amounts to about 15 $\mu\Omega$ cm, it is stable beyond 1000 °C and has the cubic CaF_2 structure with a mismatch of only -1.2% compared to Si. Several techniques exist for producing silicide films on (111) Si, for example, molecular-beam epitaxy (MBE) and ion-beam synthesis (IBS). Unfortunately, the fabrication is more complicated for the more interesting (100) surface. Until now IBS remains the only successful process. It has already been applied for producing a permeable base transistor and low resistance contacts. It should be possible to use this method for creating metal base transistors and buried interconnectors in three-dimensional circuits for VLSI (very large scale integration).

As already mentioned, the quality of the interfaces should be as good as possible. Therefore one needs a probe which can give quantitative information on the outer and inner interfaces. Among the questions to be answered are the following: Which types of atoms lie immediately at the border, what is their coordination, and what are the interatomic distances? Questions like these and related ones about the deviation from such properties caused by defects etc. are not within the scope of this work.

A totally different type of question corresponds to statistical disorder in the interface region which can be summarized under the notion roughness. In detail one has to determine the correct probability density function for the interface position in the direction of the surface normal. This mostly leads to a Gaussian distribution. Thereafter the spread in the interface position can be evaluated. X-ray reflectivity under grazing incidence conditions is a well-established technique to investigate this spread in the position of outer and inner interfaces without destroying the sample.[1] As we will show in this paper this technique can decide between interface forms with only little differences.

In addition it should be interesting to look for the shape of the interfaces in the lateral direction. That mainly concerns the character of the interface: Does it have a jagged form or is it more like smooth valleys and hills? Second, one wants quantitative information about the average distance—a correlation length—over which the main characteristics of the interface do not vary. These answers can be given by x-ray diffuse scattering under grazing incidence conditions as several authors recently have shown.[2-4] Besides, Weber and Lengeler, and Birken demonstrated that the results can be compared with other experimental techniques, such as scanning force microscopy, optical and mechanical scanning.[4,5]

In this work we have extended the investigation of diffuse scattering to buried interfaces. It should be emphasized that this extension is also valid if the difference in electron density between various layers is very large. For example, simpler solutions will not work for buried $CoSi_2$ in Si, because the electron density of the silicide is about twice the silicon value.

II. SAMPLES

IBS was first performed by White *et al.* to produce single crystalline buried layers of $CoSi_2$ in silicon.[6] For a review about IBS the reader is referred to the recent paper of Mantl.[7]

Our samples were prepared by implantation of $^{59}Co^+$ ions into silicon wafers of floating zone type with an EATON NV-3209 ion accelerator. Dose and energy of the cobalt ions determined the layer depth and thickness. The substrates were held at elevated temperatures (350 °C) to prevent amorphization. They were tilted by 7° to avoid channeling. Subsequently a two-step annealing

 ©1993 The American Physical Society

TABLE I. Results of the specular reflectivity and the diffuse scattering. The error of the fit values is of the order of the last nonzero digit. The index 1 corresponds to the surface, index 2 to the upper silicide interface, and index 3 to lower silicide interface. σ is the rms roughness, ξ the lateral correlation length of the roughness. h is a measure for the interface shape, $0<h<1$, small values mean that the interface is jagged, and large values that it is smooth. ρ is the mass density.

Energy (keV)		200			30
Dose (cm^{-2})		2×10^{17}			4.5×10^{16}
Surface		(100)		(111)	(111)
sample	1	2	3	4	5
annealing	As-implanted	Furnace	RTA	Furnace	RTA
Si thickness (Å)	820	1070	1067	1030	161
$CoSi_2$ thickness (Å)		640	750	692	166
σ_1 (Å)	13.9	40	19.5	26.2	16.5
σ_2 (Å)	200	24	29.2	16.3	2.6
σ_3 (Å)		60	23.3	9.8	6.1
ξ_1 (Å)	26	1300	1500	1700	
ξ_2,ξ_3 (Å)	220	2100	1500	3600	
h_1	0.8	0.3	0.9	0.6	
h_2,h_3	0.3	0.1	0.2	0.2	
$\frac{\Delta\rho}{\rho}$ Si	+9%	−3%	−3%	−3%	
$\frac{\Delta\rho}{\rho}$ $CoSi_2$	−24%	−7%	−16%	−8%	−10%

process was performed to obtain good crystalline quality and sharp interfaces. Prior to this, 200 nm of SiO_2 were deposited onto the surface to prevent the creation of holes in the top silicon layer during the temper process. Two kinds of annealing procedures were practiced. In the first a tube furnace with high vacuum (10^{-7} torr) was used. The samples were kept at 600 °C for one hour and subsequently at 1000 °C for half an hour. The second procedure—rapid thermal annealing (RTA)—took place in a rapid thermal processor (AET RV-1002) in floating high-purity argon. Here annealing for 10 s at 750 °C and 30 s at 1150 °C led to the best results.

For our x-ray study we compared three samples with the technically relevant (100) surface, one as implanted (sample 1) and two with each of the annealing processes (samples 2 and 3). In addition two more samples with a (111) surface were examined: sample 4 was prepared as sample 2, sample 5 was implanted with much lower dose and energy to create a very thin layer.[8] Their preparation led to a much higher degree of perfection. These (111) samples can be used to show the possible future improvements for the (100) surface. A summary of the parameters of the preparation of the five samples is displayed in Table I.

III. THEORY

A. Specular reflectivity

The x-ray reflectivity at grazing incidence for multilayer systems was first described by Parrat.[1] He showed that it is adequately explained by a recursive application of the Fresnel equation (for the geometry see Fig. 1).

$$R_{l-1}(d_{l-1})=\frac{r_{l-1,l}+R_l(d_l)e^{-2ik_{z,l}d_l}}{1+r_{l-1,l}R_l(d_l)e^{-2ik_{z,l}d_l}} . \quad (1)$$

Here $R_l=E_l^R/E_l^T$ is the ratio of outgoing to incoming electric wave amplitudes whose absolute square gives the reflected intensity. In each layer of thickness d_l the momentum transfer normal to the sample surface can be extracted from the law of refraction

$$k_{z,l}=k_l\sin\theta_l\approx k_0[\sin^2\theta_0-2(\delta_l+i\beta_l)]^{1/2} ;$$

θ_0: glancing incidence angle; $n_l=1-\delta_l-i\beta_l$: complex index of refraction.

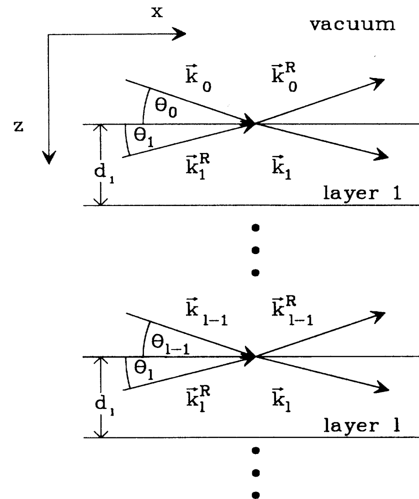

FIG. 1. X-ray geometry for a multilayer system.

$$r_{l-1,l}=\frac{k_{z,l-1}-k_{z,l}}{k_{z,l-1}+k_{z,l}}$$

gives the Fresnel reflectivity of a single interface. The roughness of the interfaces can be introduced by replacing the Fresnel equation by expressions describing the reflectivity of a rough interface. In the following we calculate the resulting reflectivity for two different analytical forms of the interface roughness $P(z)$.

(1) Névot and Croce[9] have shown the result for a Gaussian interface roughness, i.e., the probability density function of the interface position is

$$P_{\mathrm{Gauss}}(z)=\frac{1}{\sqrt{2\pi}\sigma_l}e^{-z^2/2\sigma_l^2}$$

and the resulting variation of the refraction index follows

$$n_{\mathrm{Gauss}}(z)=\frac{n_l+n_{l-1}}{2}+\frac{n_l-n_{l-1}}{2}\,\mathrm{erf}\left[\frac{z}{\sqrt{2}\sigma_l}\right]$$
$$\approx\frac{n_l+n_{l-1}}{2}+\frac{n_l-n_{l-1}}{\sqrt{2\pi}}\left[\frac{z}{\sigma_l}-\frac{1}{6}\left[\frac{z}{\sigma_l}\right]^3\pm\cdots\right]. \quad (2)$$

The reflection coefficient turns out to be

$$r_{l-1,l}^{\mathrm{rough,Gauss}}=r_{l-1,l}e^{-2\sigma_l^2k_{z,l-1}k_{z,l}} \quad (3)$$

in the limit $\sigma_l k_{z,l}<1$. Here σ_l is the root-mean-square roughness of the lth interface. This has been proved by Sinha *et al.*[2] in a different approach within the so-called distorted-wave Born approximation (DWBA) and more recently by Pynn.[3]

(2) Alternatively one can assume that the probability density function is

$$P_{\tanh}(z)=\frac{1}{\sqrt{2\pi}\cosh^2(\sqrt{2/\pi}z/\sigma_l)}.$$

The following interface form results:

$$n_{\tanh}(z)=\frac{n_l+n_{l-1}}{2}+\frac{n_l-n_{l-1}}{2}\tanh\left[\left[\frac{2}{\pi}\right]^{1/2}\frac{z}{\sigma_l}\right]$$
$$\approx\frac{n_l+n_{l-1}}{2}+\frac{n_l-n_{l-1}}{\sqrt{2\pi}}\left[\frac{z}{\sigma_l}-\frac{2}{3\pi}\left[\frac{z}{\sigma_l}\right]^3\pm\cdots\right]. \quad (4)$$

This is very similar to the error function profile [Eq. (2)] as can be seen in Fig. 2. The asymptotic limit for $z\rightarrow\pm\infty$ is identical and the power series expansion near the interface ($z=0$) is the same up to second order. Even the difference between the third-order terms is only 20%. This profile has the advantage that the Helmholtz equation for the electromagnetic fields

$$\Delta E+k^2n^2(z)E=0 \quad (5)$$

can be solved analytically, that means without the limitation $\sigma_l k_{z,l}<1$ which usually is made in the DWBA:[10,11]

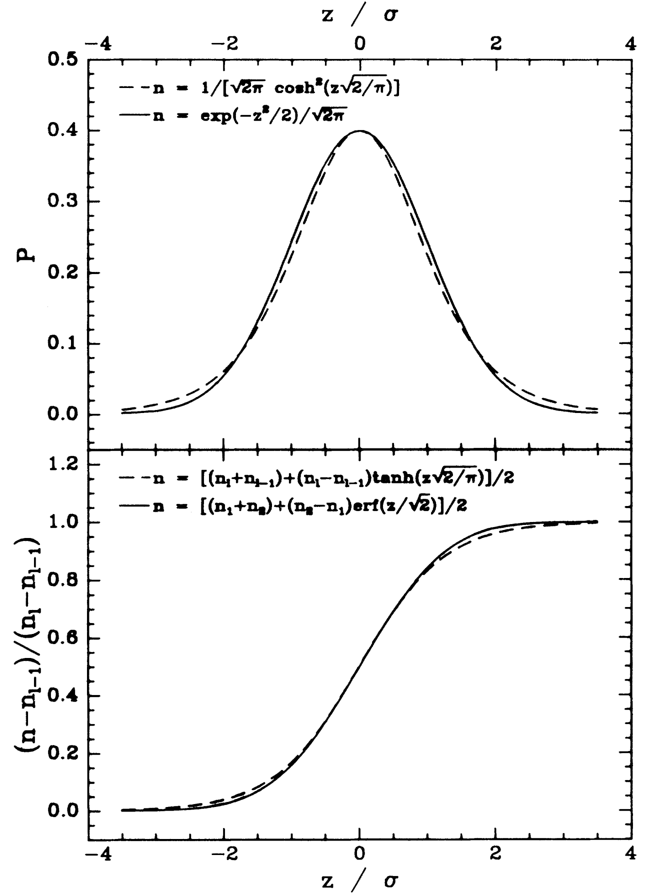

FIG. 2. Roughness models. Top: probability density functions. Bottom: variation of the index of refraction.

$$r_{l-1,l}^{\mathrm{rough,tanh}}=\frac{\sinh[(\pi/2)^{1.5}\sigma_l(k_{z,l-1}-k_{z,l})]}{\sinh[(\pi/2)^{1.5}\sigma_l(k_{z,l-1}+k_{z,l})]}G\ , \quad (6)$$

with

$$G=-\frac{\Gamma[2i\sqrt{\pi/2}\sigma_l k_{z,l-1}]}{\Gamma(-2i\sqrt{\pi/2}\sigma_l k_{z,l-1})}\times\frac{\Gamma[-i\sqrt{\pi/2}\sigma_l(k_{z,l-1}+k_{z,l})]}{\Gamma[i\sqrt{\pi/2}\sigma_l(k_{z,l-1}+k_{z,l})]}\times\frac{\Gamma[-i\sqrt{\pi/2}\sigma_l(k_{z,l-1}-k_{z,l})]}{\Gamma[i\sqrt{\pi/2}\sigma_l(k_{z,l-1}-k_{z,l})]}.$$

The factor G influences the phases of the electromagnetic fields. Nevertheless the calculation of the reflectivity would be greatly simplified if this factor could be approximated by $G\approx1$. To check the influence of G we have calculated the reflectivity for a buried silicide system by simulating the roughness with a step function which approaches the hyperbolic tangent profile. By this we got a numerical solution of the Helmholtz equation [Eq. (5)]. From the comparison with the calculation of the

reflectivity by Eq. (6) with $G=1$ up to roughnesses of $\sigma=100$ Å we conclude that we can omit this factor for our specific samples. This approach is also supported by Hamilton and Pynn.[12]

B. Diffuse scattering

To get information about the lateral structure of the samples through x-ray scattering, it is necessary to have a momentum transfer q_r in the plane of the sample surface. One possibility of doing this is to place the detector at one distinct setting and then to rotate the sample. By this one gets the specular ridge when the incident angle equals the exit angle. Its intensity can be calculated by the Parrat formalism. Underneath the specular ridge there is diffuse scattering whose specific shape depends on the realization of the interface. Unfortunately the diffuse intensity will be strongly modified by the multiple scattering at the interfaces which gives rise to Yoneda wings.[13] A method to overcome this problem was formulated by Vineyard within the DWBA.[14] In short the incoming x rays will penetrate into the sample in a way which can be described within the Fresnel formalism. This distorted wave then undergoes the scattering by the departure of the density from that of the average in the interface region. Application of the reciprocity theorem in optics leads to

$$I \propto |t^i|^2 S |t^f|^2 \ . \tag{7}$$

t^i and t^f are the Fresnel coefficients for transmission of the incoming and outgoing x rays. The formalism has been worked out by Sinha *et al.* for the diffuse scattering underneath the specular ridge of total external reflection.[2] They got the following form for the structure factor of the diffuse scattering, in which account has been taken of the poor instrumental resolution in the direction normal to the scattering plane:

$$S(q_{z,l}) = \frac{e^{-(\sigma_l^2/2)[(q_{z,l})^2+(q_{z,l}^*)^2]}}{|q_{z,l}|^2} \times \int_0^\infty \cos(q_r r)[e^{|q_{z,l}|^2 C_l(r)}-1]dr \ . \tag{8}$$

Here $C_l(r)=\sigma_l^2 e^{-(r/\xi_l)^{2h_l}}$ is a particular choice of the height-height correlation function, $q_r=k_r^f-k_r^i$ the in-plane momentum transfer, and $q_{z,l}=k_{z,l}^f-k_{z,l}^i$ the out-of-plane momentum transfer. The parameters ξ_l and h_l describe the lateral form of the interface roughness of the lth layer. ξ_l is the "cutoff" length introduced by Sinha *et al.*[2] It plays the role of a length scale within the rough interface. h_l can vary between 0 and 1 and tells how fast the position of the interface starts to differ from its initial value. Small h_l means that the interface remains in a narrow interval for long lateral ranges but that the interface is rather jagged. Large h_l implies that the interface loses memory of its initial position more rapidly but its character is much smoother (see also Chiarello *et al.*[15]).

The DWBA becomes wrong at large Q in the approximation of Sinha *et al.* of the diffuse scattering because of the use of incorrect eigenfunctions. This is already stated by the authors themselves. Pynn avoids this problem by assuming that he knows the eigenfunctions of the rough surface. By this he finds that the transmission of the outgoing wave $t_{l-1,l}^f$ has to be calculated by the transmission for the rough surface rather than that for the smooth one. He has not explicitly formulated the transmission for the rough surface and says that one has to use $t_{l-1,l}^f=1+r_{l-1,l}^{\text{rough}}$ instead of $t_{l-1,l}^f=1+r_{l-1,l}$.[3] Névot and Croce do not give such an expression, either.[9] Pynn also mentions that this relation obviously violates the reciprocity theorem in optics. His very pragmatic recommendation is to use the original result of Sinha *et al.* as long as it works to explain the experimental data.

To calculate the diffuse interface scattering from multilayer systems one further modification must be introduced. As was shown in Sec. III A, the interference of the scattered waves from the different interfaces leads to a modulated Fresnel reflectivity which could be described by a recursive formalism. This suggests use of a similar formalism for the transmission to account for the interference of the scattering at different interfaces. If one follows the same procedure as Parrat for the reflectivity, i.e., the electromagnetic fields have to be continuous at the interfaces, one gets the following recursive formula:

$$T_l = \frac{E_l^T}{E_0^T} = \frac{t_{l-1,l}e^{-ik_{z,l-1}d_{l-1}}}{1+r_{l-1,l}R_l(d_l)e^{-2ik_{z,l}d_l}} T_{l-1} \tag{9}$$

(see Refs. 16 and 17). Here R_l again is the recursion relation of Parrat [Eq. (1)] and the Fresnel coefficients r_l and t_l for the smooth interfaces may be replaced by those for the rough ones. Equation (9) can be used to calculate the electromagnetic fields in each layer dependent on incident and exit angle on the sample. The free parameters can be extracted from a reflectivity experiment (see Sec. III A). The T^i, T^f must replace the t^i and t^f in Eq. (7). Furthermore each interface must be described by its own structure factor (sum over layers):

$$I \propto \sum_l |T_l^i|^2 S_l |T_l^f|^2 \ . \tag{10}$$

It should be mentioned that so far we only have taken into account the incoherent diffuse scattering of each interface. This means that the different interfaces are totally uncorrelated. As Sinha[18] and Sanyal *et al.*[19] have reported, this is not correct if the samples have a so-called conformal roughness. This means that the height functions describing neighboring layers are not independent. Such a situation occurs, e.g., when coating a rough surface with a thin film. If the experiments cannot be explained with the incoherent scattering alone then the interference between the diffuse scattering of the different interfaces definitely must be included.

IV. EXPERIMENT

Most of the data collection was done at the National Synchrotron Light Source (NSLS) at Brookhaven National Laboratory at beam line X22B. It is a four-circle diffractometer with focusing mirror and Ge (111) monochromator. While the wavelength of a rotating anode is

restricted to discrete values, the synchrotron offers the advantage of a free choice in addition to the high brilliance. In order to minimize the absorption by the Co atoms of the samples, the wavelength $\lambda = 1.65$ Å was selected, a value just above the K absorption edge of Co. Thus information about the interface between silicide and substrate is attainable. Some of the reflectivity data also were collected with a two-circle diffractometer with the wavelengths 1.540 56 and 0.7109 Å (Cu $K\alpha_1$ and Mo $K\alpha_1$ radiation from a rotating anode).

V. EXPERIMENTAL RESULTS

Four types of x-ray measurements were performed on the five samples.

(1) All investigations started with a reflectivity study at grazing incidence, which means that the incidence angle was set equal to the exit angle. The specular ridge is superposed by diffuse scattering, which has to be subtracted. Otherwise the subsequent analysis would give incorrect values for the interface roughness.[2]

(2) The setting of incident and exit angle was detuned to measure the so-called longitudinal diffuse scattering. This means the sample angle was set to a value significantly outside of the width of the resolution function of the diffractometer. The intensities from this scan were subtracted from the reflectivity curve to get the true specular reflectivity. This is justified because the diffuse scattering is only slowly varying with Q. The following experimental data (Figs. 3–5) are always corrected for this diffuse scattering. This leads to a greater average slope of the reflectivity and correspondingly larger roughness values than would have been obtained without this procedure. All of the longitudinal diffuse scattering scans show oscillations which nearly all can be explained by the recursive formalism of Eq. (9). Beyond this there are only weak hints of additional oscillations. So we have no evidence for conformal roughness as introduced by Sinha and Sanyal *et al.*[18,19]

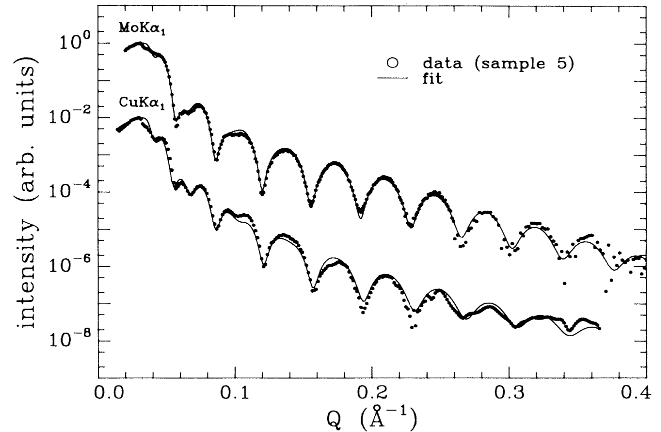

FIG. 4. Specular reflectivity of sample 5. The data were taken at a rotating anode at two different wavelengths.

(3) Since the longitudinal diffuse scans are not sensitive to the lateral structure of the interfaces transverse scans have been carried out (Fig. 6). This was done by placing the detector at a fixed position (0.8°) and only moving the sample. To analyze these transverse data, one needs additional knowledge about the samples, such as, for example, the layer thicknesses, the index of refraction, and the roughnesses. This information can be obtained from the analysis of the specular data.

So one obviously has to start with a complete interpretation of the specular scattering. At this point a general remark shall be made. Our samples are small in comparison to the x-ray beam width at grazing incidence angles. Therefore the footprint of the beam on the sample must be calculated. The result is a sine slope of the reflectivity below the critical angle. This must be done quite carefully because this correction also influences the value one gets for the surface roughness. With the knowledge of

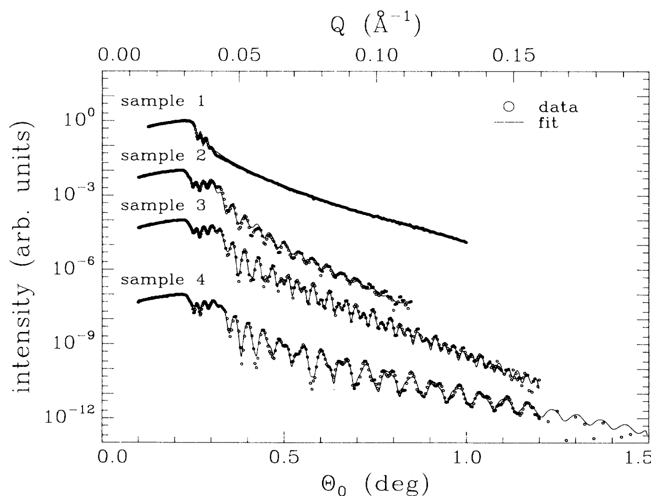

FIG. 3. Specular reflectivity. Sample 1: (100) as implanted; sample 2: (100) with furnace annealing; sample 3: (100) with RTA; and sample 4: (111) with furnace annealing. The data were taken at the NSLS.

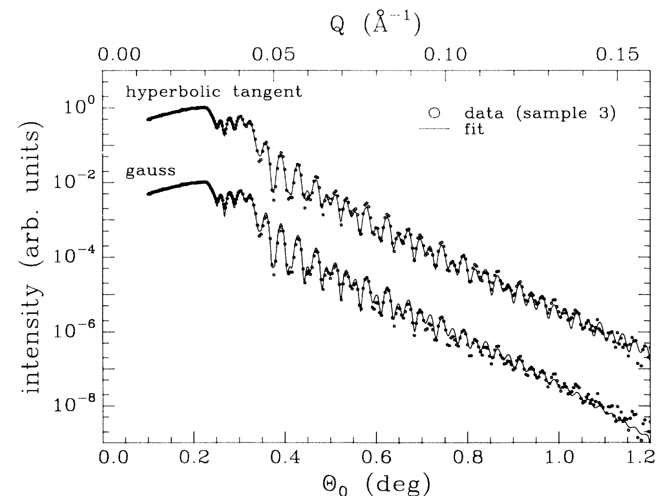

FIG. 5. Reflectivity of sample 3: Comparison of the hyperbolic tangent and Gaussian interface.

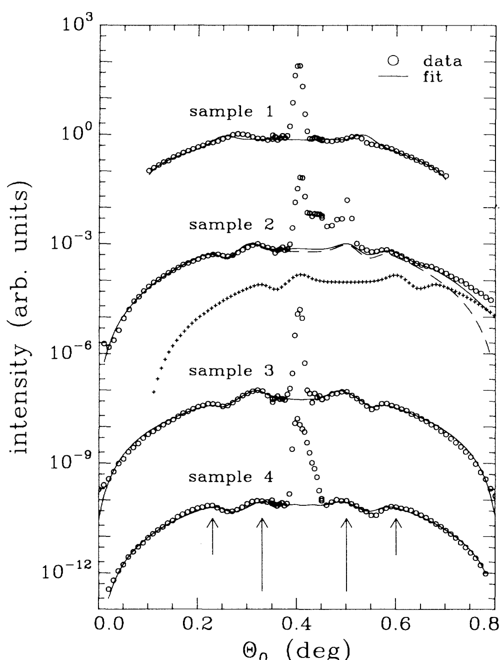

FIG. 6. Diffuse scattering of samples 1–4. The data were taken at the NSLS. The short arrows mark the positions of the Si Yoneda wings, the long ones that of $CoSi_2$. Sample 2 shows several specular peaks (sample mosaic). The dashed line represents the fit to the diffuse scattering of the most prominent peak and the crosses that to the second largest. The sum of them (line) significantly improves the fit.

the δ_l, β_l, d_l, and σ_l from the reflectivity one can start with the analysis of the diffuse scattering. As we have concluded from the general form of the longitudinal diffuse scattering the coherent diffuse scattering can be neglected. But, as the fitting of the data has shown, one needs two independent correlation functions (that means different ξ_l, h_l): The first one for the surface and the second one for the buried interfaces (identical for both interfaces). This is not surprising because their formation must be quite different. The surface is only disturbed during the implantation and the buried interfaces can drastically diminish their interface energy by planarization during the annealing. Otherwise it is not possible to get such pronounced dips between the Yoneda wings of Si and $CoSi_2$ (marked by arrows in Fig. 6). In contrast to the results of Weber and Lengeler[4] no significant influence of the replacements of the $t^i_{l-1,l}$, $t^f_{l-1,l}$ against that of the rough ones can be reported. The quantitative explanation is obtained on the basis of Eq. (9) which recursively uses the rough reflection coefficients $r^{\text{rough}}_{l-1,l}$. So the influence of the replacement of $t_{l-1,l}$ by $t^{\text{rough}}_{l-1,l}$ cannot be very large.

(4) The last experiment was the grazing incidence diffraction[20] (GID) which has been partly reported in an earlier short paper.[21] A complete report is in preparation. GID was done to prove the single crystallinity of the layers and their quality.

A. (100) surface

The main interest was devoted to the (100)-surface samples because in this case IBS is the only technique to produce buried single crystalline $CoSi_2$ layers. The first three data sets in Fig. 3 show the specular reflectivities of Si with (100) surface after Co implantation. At the top the as-implanted state is displayed (sample 1). From the average slope it is qualitatively clear that the surface roughness is not very high. In contrast to that the interfaces to the $CoSi_2$ layer must be very rough because only very few oscillations from the Si top layer are visible. They vanish just above the critical angle of the silicide, that means just when the x-ray beam begins to penetrate into the $CoSi_2$ layer. In addition it is obvious that the silicide cannot have reached its nominal mass density: Its critical angle is only weakly visible although the electron densities of Si and $CoSi_2$ differ by a factor of 2. This is confirmed by the figures obtained by the fit of the data with Eqs. (1) and (6) as can be seen in Table I. It should be underlined that the interface roughness of 200 Å is far beyond the value limiting the validity of the formalism of Névot and Croce. As expected, the mass density is below the values for pure Si and $CoSi_2$ which means that there are Si and $CoSi_2$ precipitates in each layer. This can also be seen on TEM (transmission electron microscopy) images of the as-implanted state.[7] Figure 6 shows the corresponding diffuse-scattering data. We note that the quality of the fit is not overwhelming for sample 1, which is particularly rough. But nevertheless lateral correlation lengths of $\xi_1=26$ Å for the surface and of $\xi_{2,3}=220$ Å for the interfaces between Si and $CoSi_2$ seem to be quite reasonable as a comparison with the above-mentioned TEM data shows.

The reflectivity of sample 2 proves that the furnace annealing takes care of the planarization of the buried interfaces. A visible sign is the larger range of the oscillations. Otherwise the average slope of the reflectivity implies an increase of the surface roughness. As can be seen in Table I the interface between silicide and the substrate seems to be rougher than the interface between $CoSi_2$ and the top layer.

The critical angle of Si has shifted to lower angles and that of $CoSi_2$ to larger ones. This means that the mass density of the layers has nearly reached the bulk values.

The specular peaks in the diffuse-scattering curve (Fig. 6) show that there are several—probably four—domains with different surface normals. All of them produce their own diffuse scattering. This is shown for the two dominant parts in Fig. 6. But nevertheless the correlation lengths along the interfaces have increased to $\xi_1=1300$ Å and $\xi_{2,3}=2100$ Å. The distance between steps is larger for the silicide interfaces than at the surface.

All of the results are at least qualitatively supported by the TEM image of a similarly produced sample (Fig. 7).

The reflectivity of sample 3 shows that the interface quality can be drastically improved by RTA. This can be seen by the third curve in Fig. 3. The oscillations are strongly modulated and extend up to larger Q values compared to those of sample 2. This is confirmed by the parameters which result from the fit (Table I). Interest-

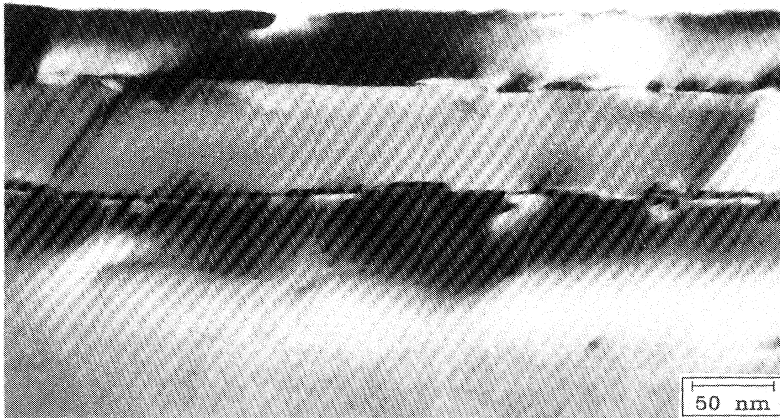

FIG. 7. TEM image of a sample with preparation similar to sample 2. The Si surface is modified due to TEM preparation and can therefore not be compared with the x-ray results. The correlation length $\xi_{2,3}=2100$ Å obtained from the diffuse scattering is of the order of the lateral distance between the steps at the interfaces. The normal roughness is of the same order as $\sigma_2=24$ Å and $\sigma_3=60$ Å. One must consider that the x rays average over a macroscopic range whereas TEM only looks at a specific microscopic area of the sample.

ingly the interface to the substrate looks smoother than the top interface of the silicide. The $CoSi_2$ density approaches closer to its bulk value, although the remaining difference is significant. The known tetragonal strain of the silicide[7] can partly explain this fact but this effect alone is too small. So there may be remaining Si precipitates or defects (vacancies) in the $CoSi_2$. As Fig. 6 displays, there is only a single well-defined domain and the correlation lengths at the interfaces amount to about the same values as for sample 2 but without any difference between the surface and the buried interfaces. Also here the results are supported by TEM (Fig. 8).

At this point a short remark shall be made about the values of h, the parameter which describes the general character of the interface. h is strongly correlated with the correlation length ξ. But generally the surface has larger values for h than the buried interfaces. This means that the surface is smoother than the silicide borders.

B. (111) surface

An additional study of a (111)-surface sample was done because the preparation of such surfaces is easier and much better developed. Immediately one recognizes from the Q range of the oscillations of sample 4 (Fig. 3) that the interface quality is better although the annealing was done by standard furnace heating. Also the correlation lengths at the interfaces seem to be larger (deduced from the diffuse scattering of sample 4 in Fig. 6). Again the distance between steps in the buried interfaces exceeds that in the surface. However, the surface roughness is not improved in comparison to the (100) surface. As for the (100) surfaces the values of the h_l again suggest that the silicide borders are more jagged than the surface.

Finally we want to show the reflectivity of one low-dose-implantation sample gained on a two-circle diffractometer at a rotating anode (sample 5). The measurement was performed at two different wavelengths (Cu and Mo target) to get more independent data because the reflectivity only shows weak modulation of the oscillations. Unfortunately, the influence of the wavelength variation is not very great. This is understandable since the layer thicknesses yield only about 160 Å (see Table I). As can be concluded from the very large Q range of the reflectivity in Fig. 4 the interfaces are much smoother than for the other samples. This can also be seen from the TEM image in Fig. 9. The discrepancy at the critical angle is not yet understood. It is observed at both wavelengths and therefore we believe that the observation is

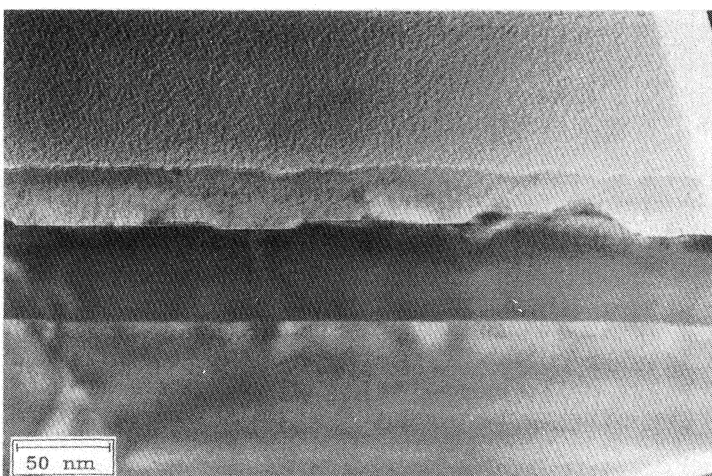

FIG. 8. TEM image of a sample with preparation similar to sample 3. As in Fig. 7, $\xi_{2,3}=1500$ Å corresponds to the lateral distance between the steps at the interfaces.

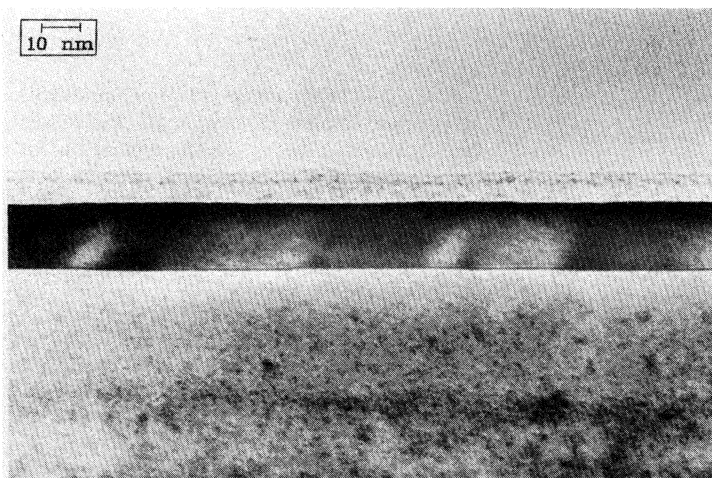

FIG. 9. TEM image of a sample with preparation similar to sample 5. The silicide interfaces seem to be perfectly flat. The x-ray reflectivity gives corresponding low values of $\sigma_2=2.6$ Å and $\sigma_3=6.1$ Å.

not accidental but reflects a feature of the sample. It shall be emphasized that the reason for this discrepancy is not a wrong value for the critical angle because its position is superposed by the first oscillation which is too high in amplitude but at the correct position in the calculation.

C. General remarks about profile sensitivity

In this section we want to compare the two interface models introduced as possible explanations of the measured reflectivities. The samples with moderate roughnesses can be fitted both with the model of Névot and Croce [Eq. (3)] and a hyperbolic-tangent-shaped transition [Eq. (6)]. Within error they yield the same values for the interface properties. Nevertheless, for large values of the momentum transfer the tanh profile works better, resulting in lower values for the least-squares sum

$$\chi^2=\sum_{i=1}^{N}\left[\frac{\log_{10}(y_i^{\text{observed}})-\log_{10}(y_i^{\text{calculated}})}{\Delta y_i}\right]^2 .$$

This can be seen by the comparison of the two curves in Fig. 5. Both show a least-squares fit with either the model Eq. (3) or Eq. (6). It is obvious that there are significant differences for large Q values, where the hyperbolic tangent profile yields the better model for these samples. Two aspects could be responsible. The first possibility is the violation of the condition $\sigma k_{z,l}<1$. This was tested by fitting the data with a model which simulated the error function with a step function consisting of 50 steps. This yielded equally good fits as with Eq. (3) for roughnesses up to about 30–40 Å. So the small difference in the profile form (Fig. 2) should be the main reason for the better fits. We conclude that x-ray reflectivity responds very sensitively on the shape of the profile.

VI. CONCLUSIONS

Summing up the x-ray part we presented an evaluation of the diffuse scattering from multilayer systems. This was achieved by combining the idea of the DWBA with the Parrat formalism. Along these lines information about the lateral interface structure is obtained. Furthermore, standard reflectivity measurements lead to quantitative data for the direction normal to the surface of the samples: quantitative results for interface roughnesses and layer thicknesses. The interface profile has been described with an error function (Névot-Croce) and a hyperbolic tangent. It was demonstrated that the x-ray measurements are very sensitive to the shape of the profile if the reflectivity extends to large enough Q ($1/\sigma<k_{z,l}$). All data are in qualitative agreement with TEM images.

Our measurements have shown that IBS is able to produce buried single crystalline $CoSi_2$ layers in (100) silicon with thicknesses beyond the limit of pseudomorphic growth. For the (111) orientation very smooth silicide interfaces can be achieved. For high ion doses the rms values amount to about $\sigma=10$ Å with a correlation length of $\xi=3600$ Å. For lower doses the interfaces are still more perfect: approximately $\sigma=5$ Å. The (100) samples have about twice as rough interfaces with corresponding shorter correlation lengths. In general rapid thermal annealing provides better interface qualities than standard furnace heating.

ACKNOWLEDGMENTS

This project was carried out with funding from the Bundesministerium für Forschung und Technologie under Contract No. 05401ABI2. The measurements at Brookhaven National Laboratory were generously supported by the United States Department of Energy under Contract No. U.S. DOE DE-AC02-76CH00016. One of us (D.B.) is indebted to L. D. Gibbs, S. K. Sinha, and S. Shapiro for their hospitality at BNL. We want to thank B. Asmussen, S. Harm, M. Müller, and M. Tolan for discussion.

[1]L. G. Parrat, Phys. Rev. **95**, 359 (1954).

[2]Sunhil K. Sinha, E. B. Sirota, S. Garoff, and H. B. Stanley, Phys. Rev. B **38**, 2297 (1988).

[3]Roger Pynn, Phys. Rev. B **45**, 602 (1992).

[4]Wolfgang Weber and Bruno Lengeler, Phys. Rev. B **46**, 7953 (1992).

[5]Hans-Gunther Birken, Ph.D. thesis, Universität Hamburg, 1991.

[6]A. E. White, K. T. Short, R. C. Dynes, J. P. Garno, and J. M. Gibson, Appl. Phys. Lett. **50**, 95 (1987).

[7]Siegfried Mantl, Mater. Sci. Rep. **8**, 1 (1992).

[8]Rolf Jebasinski, Siegfried Mantl, L. Vescan, and Ch. Dieker, Appl. Surf. Sci. **53**, 264 (1991).

[9]L. Névot and P. Croce, Rev. Phys. Appl. **15**, 761 (1980).

[10]John Lekner, *Theory of Reflection* (Nijhoff, Dordrecht, 1987).

[11]A. V. Andreev, A. G. Michette, and A. Renwick, J. Mod. Opt. **35**, 1667 (1988).

[12]W. A. Hamilton and Roger Pynn, Physica B **173**, 71 (1991).

[13]Y. Yoneda, Phys. Rev. **131**, 2010 (1963).

[14]George H. Vineyard, Phys. Rev. B **26**, 4146 (1982).

[15]R. Chiarello, V. Panella, J. Krim, and C. Thompson, Phys. Rev. Lett. **67**, 3408 (1991).

[16]D. K. G. de Boer, Phys. Rev. B **44**, 498 (1991).

[17]J. F. Akner, in *X-Ray and Neutron Scattering,* edited by Hartmut Zabel and Ian K. Robinson (Springer-Verlag, Berlin, 1992), p. 105.

[18]Sunhil K. Sinha, Physica B **173**, 25 (1991).

[19]Milan K. Sanyal, Sunhil K. Sinha, A. Gibaud, S. K. Satija, C. F. Majkrzak, and H. Homa, in *Surface X-Ray and Neutron Scattering,* edited by Hartmut Zabel and Ian K. Robinson (Springer-Verlag, Berlin, 1992), p. 91.

[20]W. C. Marra, Peter Eisenberger, and A. Y. Cho, J. Appl. Phys. **50**, 6927 (1979).

[21]Detlef Bahr, Bernd Burandt, Metin Tolan, Werner Press, Rolf Jebasinski, and Siegfried Mantl, in *Surface X-Ray and Neutron Scattering,* edited by Hartmut Zabel and Ian K. Robinson (Springer-Verlag, Berlin, 1992), p. 187.

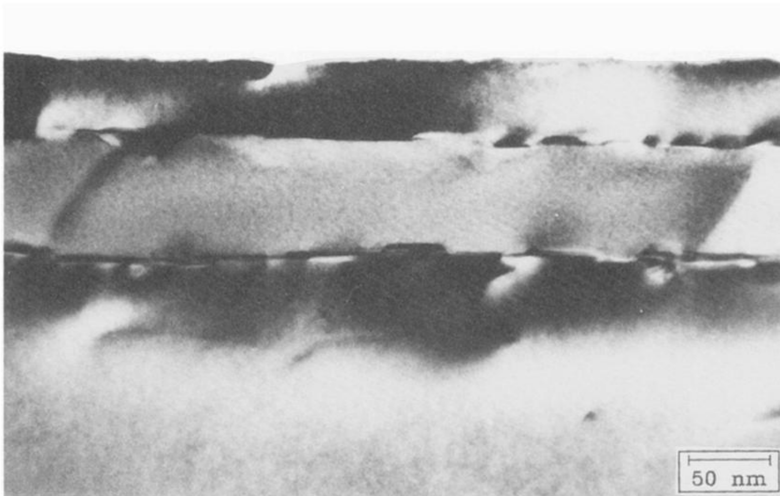

FIG. 7. TEM image of a sample with preparation similar to sample 2. The Si surface is modified due to TEM preparation and can therefore not be compared with the x-ray results. The correlation length $\xi_{2,3}=2100$ Å obtained from the diffuse scattering is of the order of the lateral distance between the steps at the interfaces. The normal roughness is of the same order as $\sigma_2=24$ Å and $\sigma_3=60$ Å. One must consider that the x rays average over a macroscopic range whereas TEM only looks at a specific microscopic area of the sample.

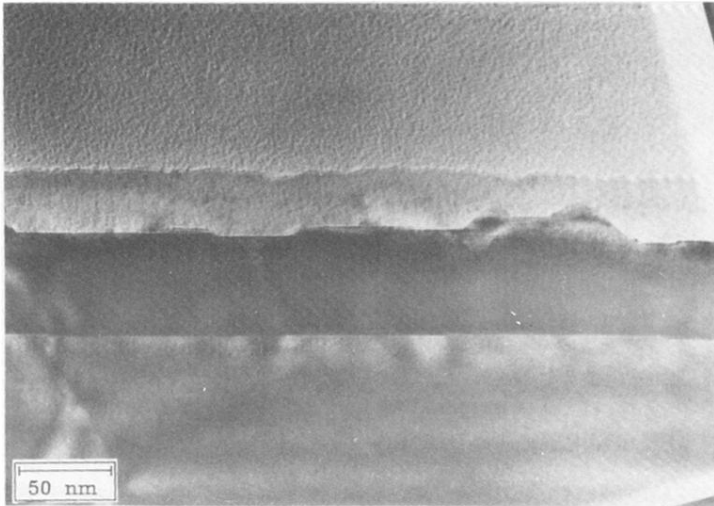

FIG. 8. TEM image of a sample with preparation similar to sample 3. As in Fig. 7, $\xi_{2,3} = 1500$ Å corresponds to the lateral distance between the steps at the interfaces.

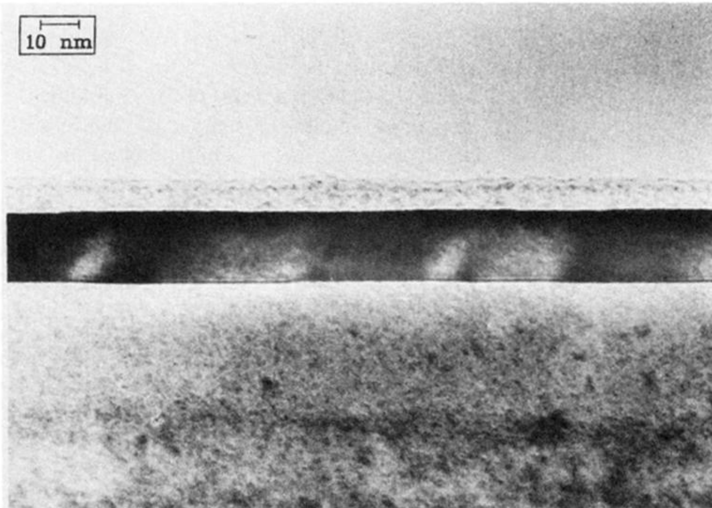

FIG. 9. TEM image of a sample with preparation similar to sample 5. The silicide interfaces seem to be perfectly flat. The x-ray reflectivity gives corresponding low values of $\sigma_2 = 2.6$ Å and $\sigma_3 = 6.1$ Å.